Applied Sciences Program
NASA Earth Science

Real-Time Spatial Estimates of Snow-Water Equivalent (SWE)

Sierra Nevada Mountains, California

February 16, 2020

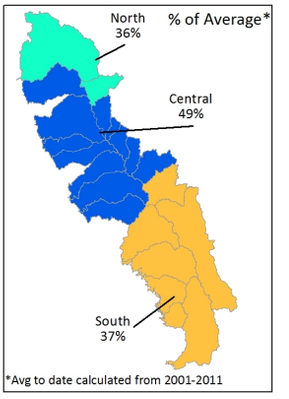

Team: Noah Molotch[1,2], Leanne Lestak[1], Keith Musselman[1], and Kehan Yang[1]
[1] Center for Water, Earth Science & Technology, Institute of Arctic and Alpine Research, University of Colorado Boulder
[2] Jet Propulsion Laboratory, California Institute of Technology
Contact: Leanne.Lestak@colorado.edu

Summary of current conditions

The regional summary map above shows the mean SWE above 5000' elevation for three major regions of the Sierra Nevada. As of February 16, regional average SWE remained below average across the Sierra, with percent of average SWE ranging from 36% in the north, 49% in the central and 37% in the southern Sierra. Detailed SWE maps (in JPG format) and summaries of SWE (in Excel tables) by individual basin and elevation band are also provided in the report. There is unusually low or no SWE at elevations below 7000 ft for this time of year. This may explain our lower basin average SWE estimates compared to the long-term average values being reported by snow pillow stations.

About this report

This is an experimental research product that provides near-real-time estimates of snow-water equivalent (SWE) at a spatial resolution of 500 m for the Sierra Nevada in California from mid-winter through the melt season. The report is released within a week of the date of data acquisition at the top of the report. A similar report covering the Intermountain West, is available and is distributed to water managers in Colorado, Utah and Wyoming.

The spatial SWE analysis method for the Sierra Nevada uses the following data as inputs:

- In-situ SWE from all operational CA snow gage sensor sites
- MODSCAG fractional snow-covered area (fSCA) data from recent cloud-free MODIS satellite images
- Physiographic information (elevation, latitude, upwind mountain barriers, slope, etc.)
- Historical daily SWE patterns (2000-2014) retrospectively generated using historical MODSCAG data and an energy-balance model that back-calculates SWE given the fSCA time-series and meltout date for each pixel
- CoCoRaHS SWE values when available and applicable

For more details on the estimation method see the *Methods* section below. Please be sure to read the *Data Issues / Caveats* section for a discussion of persistent challenges or flagged uncertainties of the SWE product.

Data availability for this report

98 snow gage sites in the Sierra Nevada network were recording SWE values out of a total of 114 sites, 16 were offline and 0 were recording zero SWE (shown in red and yellow, respectively, in Figure 6, left map).

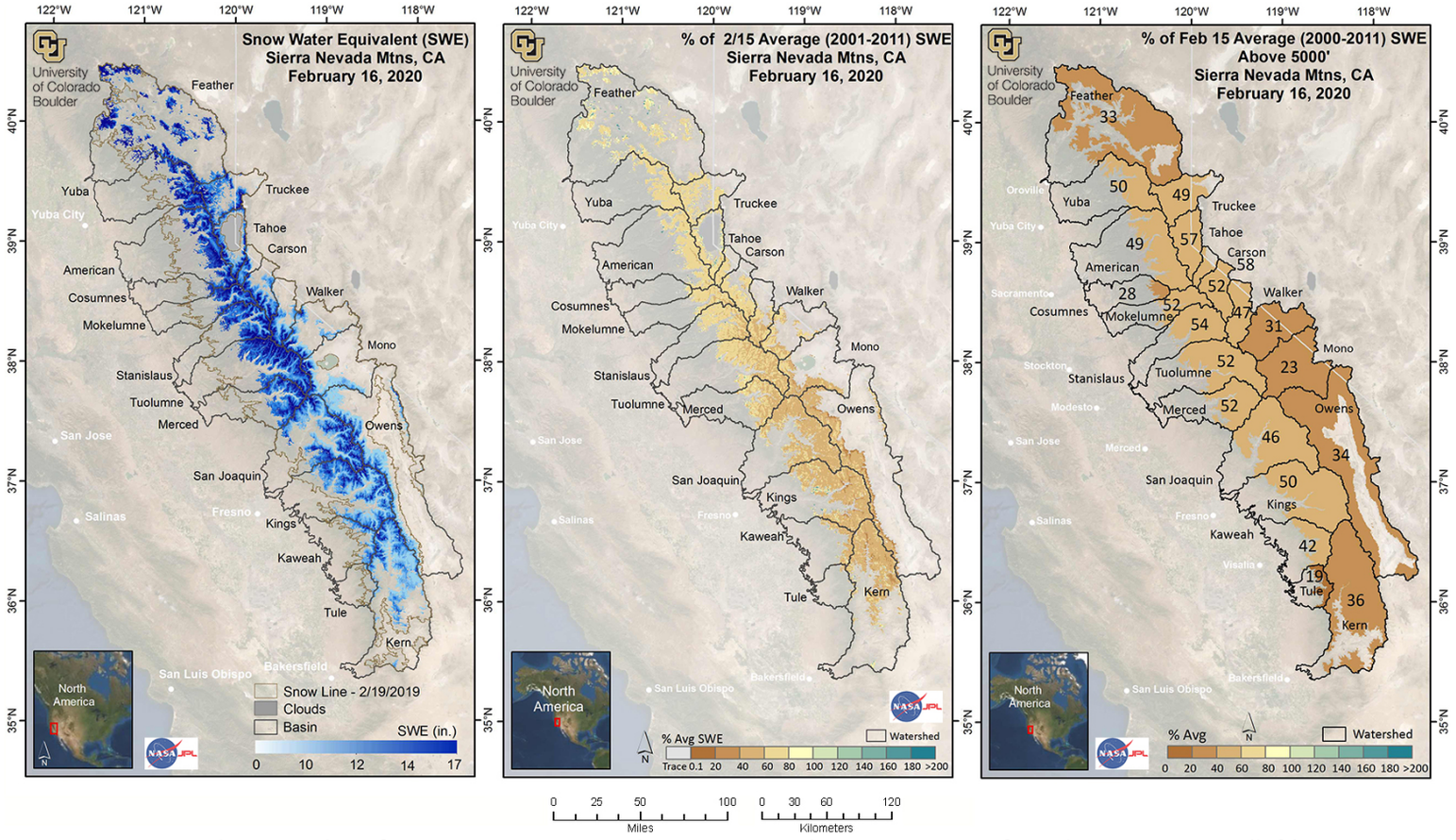

Figure 1. Estimated SWE and % of Average SWE across the Sierra Nevada. SWE amounts for February 16, 2020 (left), percent of average (2001-2011) SWE for February 16, 2020 for the Sierra Nevada, calculated for each pixel (middle) and basin-wide (right). Basin-wide percent of average is calculated across all model pixels >5000' elevation. For comparison the left map also includes the snow line for last year's February 19th report, which was at a much lower elevation than average. Our snow line this year is at a higher elevation than average. Low elevation summaries of SWE, percent of average and percent of snow-covered area are much lower most likely because of the high snow line this year.

The value of spatially explicit estimates of SWE

Snowmelt makes up the large majority (~60-85%) of the annual streamflow in the Sierra Nevada. The spatial distribution of snow-water equivalent (SWE) across the landscape is complex. While broad aspects of this spatial pattern (e.g., more SWE at higher elevations and on north-facing exposures) are fairly consistent, the details vary a lot from year to year, influencing the magnitude and timing of snowmelt-driven runoff.

SWE is operationally monitored at just over a hundred snow gage sensor sites spread across the Sierra Nevada, providing a critical first-order snapshot of conditions, and the basis for runoff forecasts from the CA DWR, NRCS, and NOAA. However, conditions at snow sensor sites (e.g., percent of normal SWE) may not be representative of conditions in the large areas between these point measurements, and at elevations above and below the range of the sensor sites. The spatial snow analysis creates a detailed picture of the spatial pattern of SWE using snow sensors, satellite, and other data, extending beyond the snow sensor sites to unmonitored areas.

Interpreting the spatial SWE estimates in the context of SNOTEL

The spatial product estimates SWE for every pixel where the MODSCAG product identifies snow-cover. Comparatively, snow sensor samples 8-20 points per basin within a narrower elevation range. Thus, the basin-wide percent of average from the spatial SWE estimates is not directly comparable with the snow sensor basin-wide percent of average. A better comparison might be made with the % of average in the elevation bands (Table 2) that contain snow sensor sites.

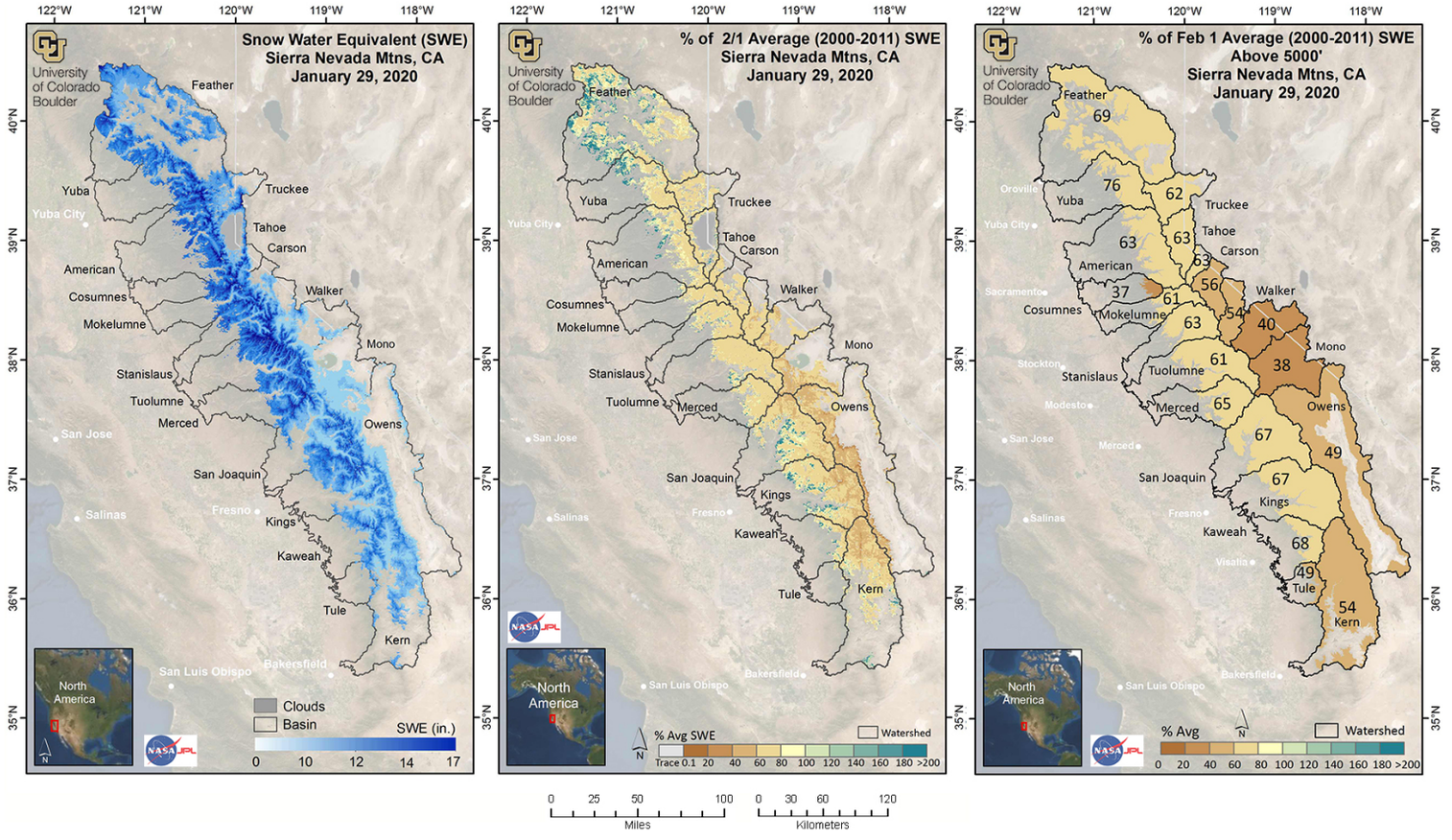

Figure 2. Estimated SWE and % of Average SWE across the Sierra Nevada. SWE amounts for January 29, 2020 (left), percent of average (2000-2011) SWE for January 29, 2020 for the Sierra Nevada, calculated for each pixel (middle) and basin-wide (right). Basin-wide percent of average is calculated across all model pixels >5000' elevation.

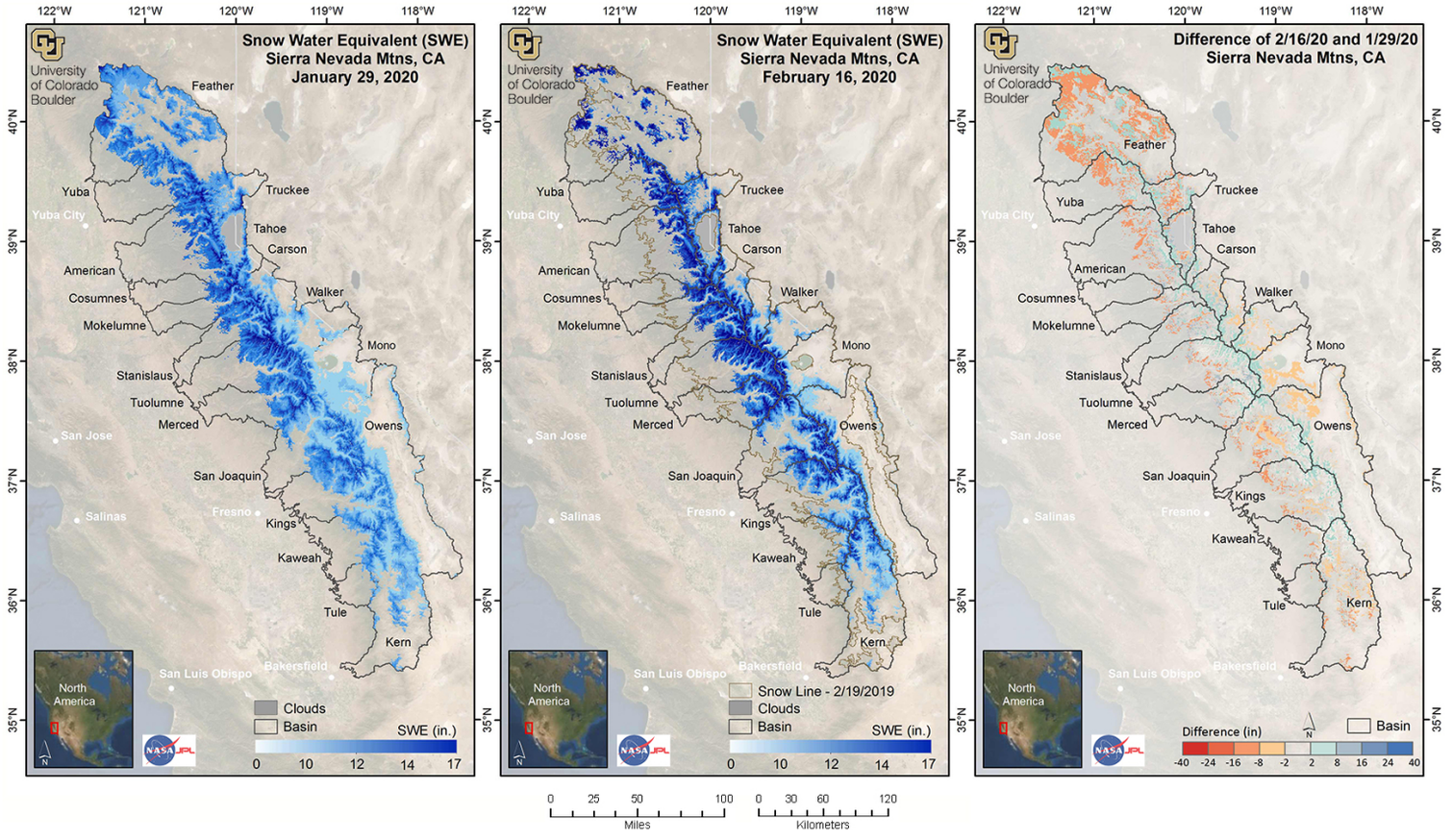

Figure 3. Estimated SWE across the Sierra Nevada, February 16, 2020. SWE amounts for January 29th (left), February 16th (middle) and the difference between February 16th and January 29th (right).

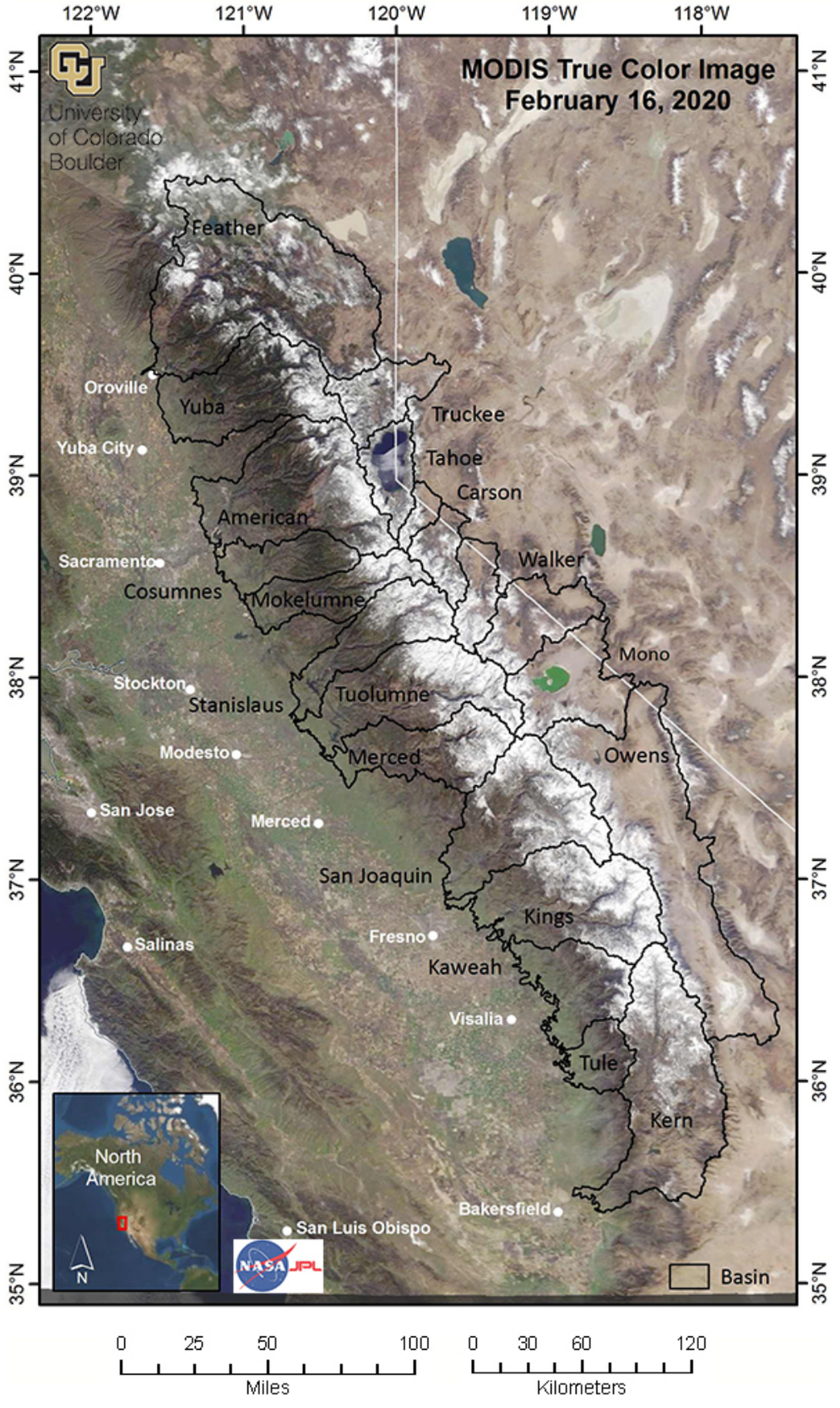

Figure 4. MODIS image, Sierra Nevada. A composite, mostly cloud-free true color MODIS image, used for the February 16, 2020 regression model run was created with February 12th (middle and north), February 13th (far north), and February 16th (the south) MODIS imagery.

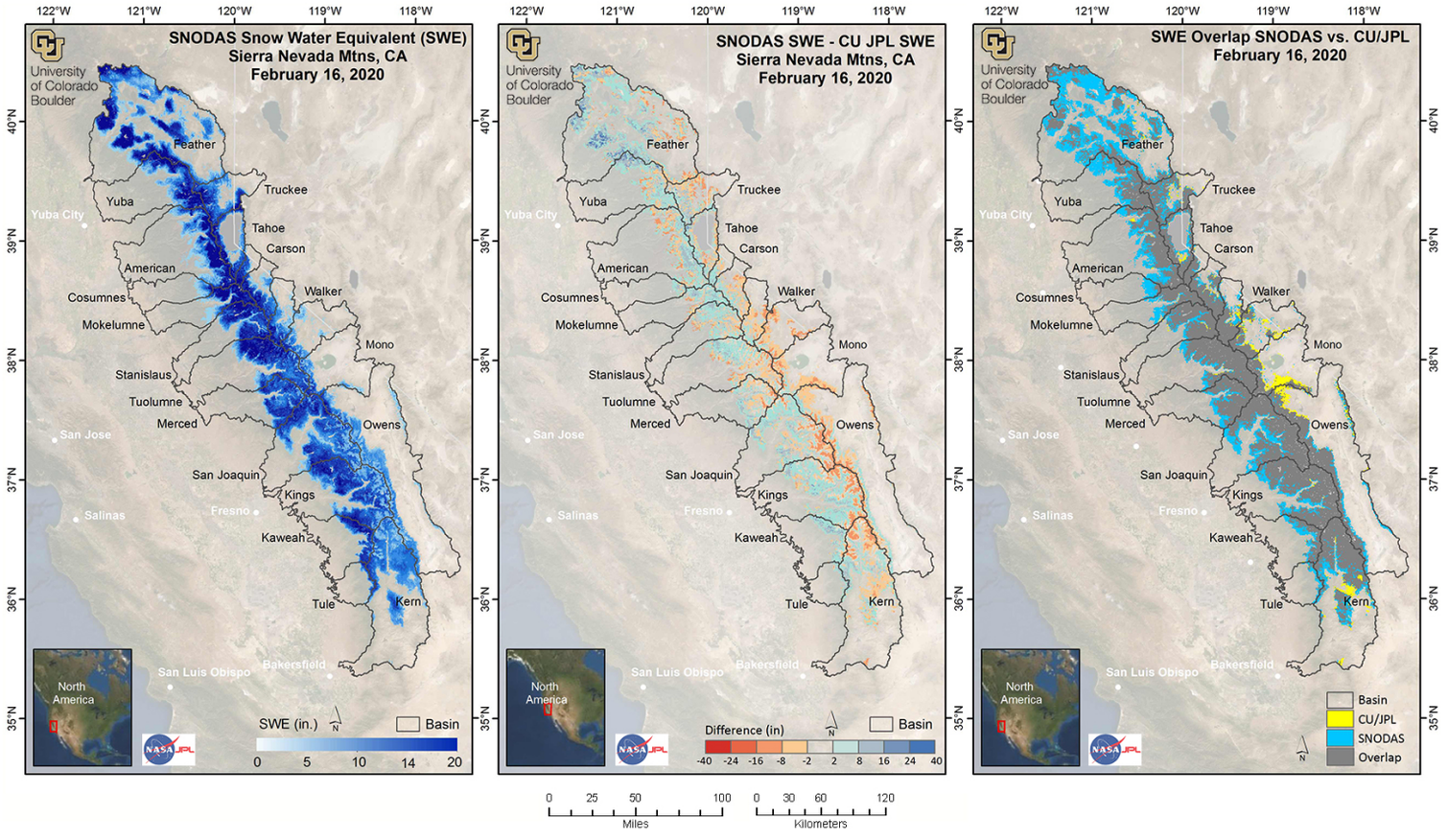

Figure 5. Comparison of CU/JPL regression SWE product and SNODAS SWE for the Sierra Nevada. The map on the left shows estimated SWE for February 16th from the NOAA National Weather Service's National Operational Hydrologic Remote Sensing Center (NOHRSC) SNOw Data Assimilation System (SNODAS). The middle map shows the difference between the February 16th SNODAS SWE estimate and CU/JPL regression SWE estimate. Red pixels denote areas where SNODAS SWE is less than CU/JPL SWE and blue pixels show areas where SNODAS SWE is higher than CU/JPL SWE. The map on the right shows the snow-cover extent of SNODAS and CU/JPL SWE estimates. Yellow pixels show where the location of CU/JPL snow extends beyond the location of the SNODAS snow extent. Blue pixels show where the SNODAS snow extends beyond the CU/JPL snow extent. Gray areas indicate regions where both products agree on the snow-cover extent.

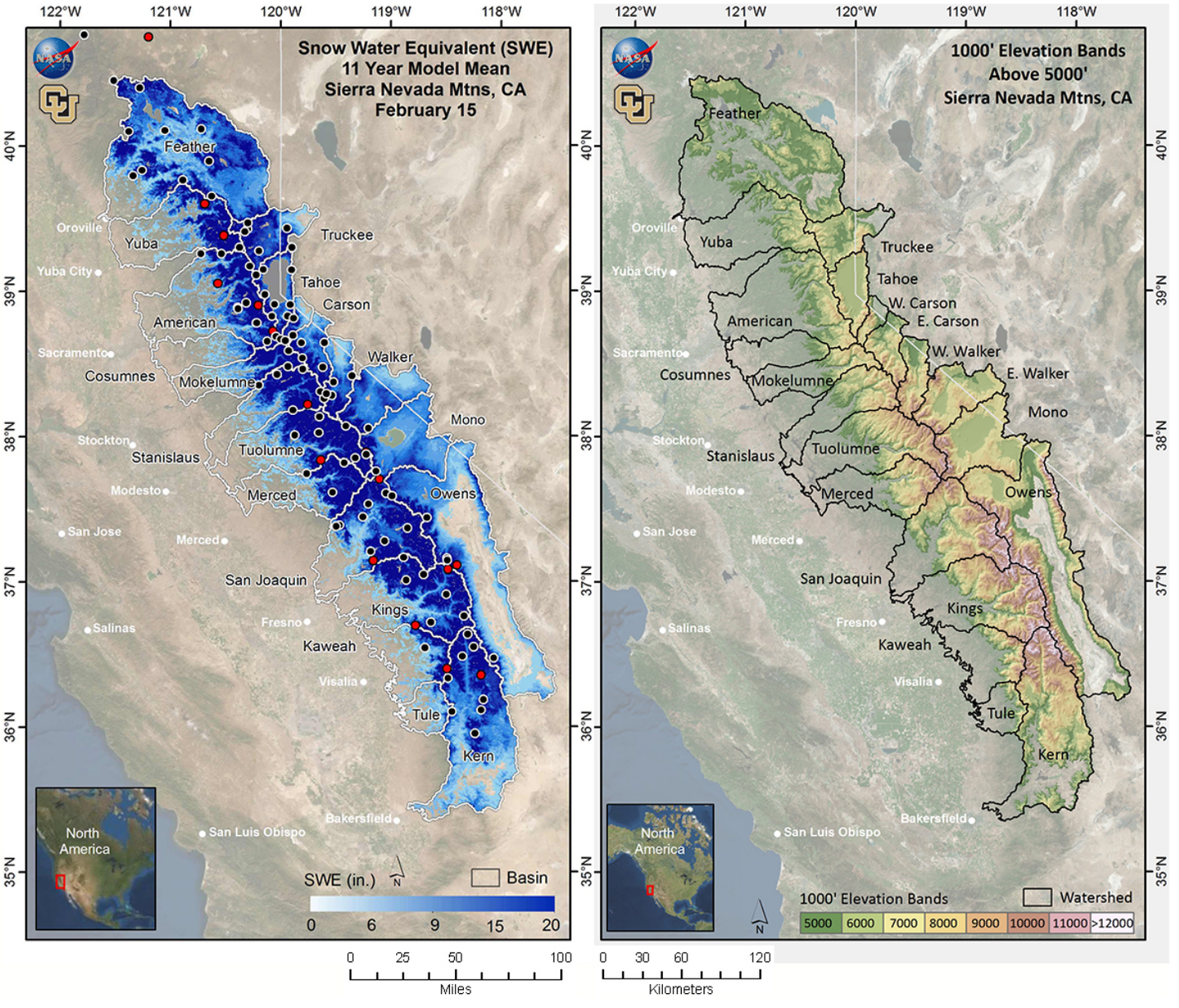

Figure 6. Historical average February 15th and Elevation Bands for the Sierra Nevada. Average SWE (2001-2011) for February 15th (left), and the Banded Elevation map (right) identifies basins used in this report (black boundaries) and 1000' elevation bands (colored shading) that match those used in Table 1 and Table 2. Map on left shows snow gage sensor sites recording SWE on January 16th (black), sites that were offline are shown in red.

Methods

The spatial SWE estimation method is described in Schneider and Molotch (2016). The method uses linear regression in which the dependent variable is derived from the operationally measured in situ SWE from all online snow sensor sites in the domain. The snow sensor SWE observations are scaled by the fractional snow-covered area (fSCA) across the 500 m pixel containing that snow sensor site before being used in the linear regression model. The fSCA is a near-real-time cloud-free MODIS satellite image which has been processed using the MODIS Snow Cover and Grain size (MODSCAG) fractional snow-covered area algorithm program (Painter, et. al. 2009, snow.jpl.nasa.gov).

The following independent variables (predictors) enter into the linear regression model:

- Physiographic variables that affect snow accumulation, melt, and redistribution, including elevation, latitude, upwind mountain barriers, slope, and others. See Figure 2 in Schneider and Molotch (2016) for the full set of these variables.
- The historical daily SWE pattern (1985-2016) retrospectively generated using historical MODSCAG data, and an energy-balance model that back-calculates SWE given the fractional Snow-Covered Area (fSCA) time series and meltout date for each pixel. See Margulis, et. al., 2016 for details. (For computational efficiency, only one image from either the 1st or 15th of

each month during the 1985-2016 period that best matches the real-time SNOTEL-observed pattern is selected as an independent variable.)

The real-time regression model for this date has been validated by cross-validation, whereby 10% of the SNOTEL data are randomly removed and the model prediction is compared to the measured value at the removed SNOTEL stations. This is repeated 30 times to obtain an average R-squared value, which denotes how closely the model fits the SNOTEL data. During development of this regression method, the model was also validated against independent historical SWE data collected in snow surveys at 9 locations in Colorado, and an intensive field survey in north-central Colorado.

Data Issues/Caveats for* January 16, 2020 – *IMPORTANT – READ THIS!

- DENSE FOREST COVER – Dense forest cover at lower elevations where snow-cover is discontinuous can cause the satellite to underestimate the snow-cover extent, leading to underestimation of SWE.
- ANOMALOUS SNOW PATTERNS – Anomalous snow years or snow distributions may cause SWE error due to the model design to search for similar SWE distributions from previous years. If no close seasonal analogue exists, the model is forced to find the most similar year, which may result in error.
- CLOUD COVER – Cloud cover can obscure satellite measurements of snow-cover. While careful checks are made, occasionally the misclassification of clouds as snow or *vice versa* may result in the mischaracterization of SWE or bare-ground.
- LOW LOOK ANGLE – When a satellite does not pass directly over a region but the area is still included within the satellite sensor's field of view, this is referred to as a low "look angle". The resulting image has lower effective resolution – this "blurry" MODSCAG data still contains useful information but may lead to overestimation of SWE near the margins of the snow-cover extent. The only applies to the February 13th image used for the far north.

List of All Known Data Issues/Caveats

- RECENT SNOWFALL – There are occasionally problems with lower-elevation SWE estimates due to recent snowfall events that result in extensive snow-cover extending to valley locations where measurements are not available. This scenario results in an over-estimation of lower- elevation SWE.
- LIMITED SNOW PILLOW DATA – When snow at the snow pillow sites melts out, but remains at higher elevations, the model tends to underestimate SWE at the under-monitored upper elevations. This issue typically occurs late in the melt season, resulting in less accurate SWE prediction at higher elevations compared to earlier in the snow season.
- CLOUD COVER – Cloud cover can obscure satellite measurements of snow-cover. While careful checks are made, occasionally the misclassification of clouds as snow or *vice versa* may result in the mischaracterization of SWE or bare-ground.
- LOW LOOK ANGLE – When a satellite does not pass directly over a region but the area is still included within the satellite sensor's field of view, this is referred to as a low "look angle". The resulting image has lower effective resolution – this "blurry" MODSCAG data still contains useful information but may lead to overestimation of SWE near the margins of the snow-cover extent.
- POOR QUALITY SNOTEL DATA – Although data QA/QC is performed, occasional SNOTEL sensor malfunction may result in localized SWE errors.
- ANOMALOUS SNOW PATTERNS – Anomalous snow years or snow distributions may cause SWE error due to the model design to search for similar SWE distributions from previous years. If no close seasonal analogue exists, the model is forced to find the most similar year, which may result in error.
- DENSE FOREST COVER – Dense forest cover at lower elevations where snow-cover is discontinuous can cause the satellite to underestimate the snow-cover extent, leading to underestimation of SWE.

Table 1. Estimated SWE by basin. *The basin-wide SWE values and averages, are across all pixels at elevations >5000'. Shown are January 29th percent of February 1st average SWE, February 16th percent of February 15th average SWE (between 2001-2011 as derived from the regression model), January 29th mean SWE, February 16th mean SWE, February 16th percent of snow-covered area, February 16th water volume (acre-feet), the change in SWE between January 29th and February 16th, the area (mi^2) inside each basin that contains data pixels (not including cloud-covered pixels, lakes or other satellite no data pixels), February 16th snow pillow data for those areas collected, summarized for each basin. The last column shows February 16th mean SWE from SNODAS*.*

Basin	1/29/20 % 2/1 Avg.	2/16/20 % 2/15 Avg.	1/29/20 SWE (in)	2/16/20 SWE (in)	2/16/20 % SCA	2/16/20 Vol (af)	1/29 thru 2/16/20 Chg. in SWE (in)	Area (mi2) > 5000'	2/16/20 Pillows	2/16/20 SNODAS* (in)
Feather	69	33	7.1	4.4	31.5	524,714	-2.7	2,239.5	15.5 (8)	7.3
Yuba	76	50	10.3	8.6	61.3	251,708	-1.7	551.5	17.4 (2)	11.7
American	63	49	8.5	8.0	59.4	364,042	-0.4	848.3	13.5 (10)	9.3
Cosumnes	37	28	2.8	2.8	21.3	14,353	0.1	94.5	NA	4.8
Mokelumne	61	52	8.4	8.9	66.2	158,821	0.5	335.7	15.9 (1)	10.9
Stanislaus	63	54	8.7	9.3	71.4	293,555	0.7	591.0	15.3 (5)	10.2
Tuolumne	61	52	8.4	9.2	69.5	470,589	0.8	960.0	11.7 (6)	9.1
Merced	65	52	8.0	8.5	68.1	254,239	0.5	563.2	12.2 (3)	8.7
San Joaquin	67	46	8.3	7.7	68.2	520,036	-0.6	1,270.5	10.6 (8)	7.9
Kings	67	50	8.1	7.9	75.7	531,726	-0.1	1,256.6	13.3 (6)	8.4
Kaweah	68	42	5.6	4.9	46.6	83,704	-0.8	323.5	2.8 (1)	8.0
Tule	49	19	1.9	1.3	13.5	9,877	-0.6	142.1	9.7 (1)	3.3
Kern	54	36	4.7	4.0	45.2	390,884	-0.6	1,824.7	8.6 (7)	3.4
Truckee	62	49	7.4	7.2	56.4	225,033	-0.2	587.9	11.6 (6)	6.8
Tahoe	63	57	7.8	9.1	45.3	162,154	1.3	335.2	11.2 (8)	9.3
W Carson	63	58	6.7	7.9	67.5	55,784	1.2	132.4	14.7 (2)	8.6
E Carson	56	52	6.1	6.9	59.5	156,876	0.8	428.1	10.1 (5)	6.0
W Walker	54	47	5.3	5.5	49.2	134,789	0.2	456.8	10 (5)	3.9
E Walker	40	31	3.0	3.0	29.3	133,639	0.0	848.9	5.4 (1)	1.2
Mono	38	23	2.7	2.3	23.9	129,000	-0.5	1,070.8	6.6 (1)	1.0
Owens	49	34	2.6	2.5	32.3	296,072	-0.1	2,252.4	6.9 (4)	1.5

* This is a comparison to the SNODAS (SNOw Data Assimilation System) nationwide product from the National Weather Service.

Table 2. Estimated SWE by basin and elevation band. *Elevation bands begin at 5000' and extend past the highest point in the basin. Note that the area of the highest 2-5 bands is typically much smaller than the lower bands. Shown are January 29th percent of February 1st average SWE, February 16th percent of February 15th average SWE (between 2001-2011 as derived from the regression model), January 29th mean SWE, February 16th mean SWE, February 16th percent of snow-covered area, February 16th water volume (acre-feet), the change in SWE between January 29th and February 16th, the area (mi^2) inside each basin that contains data pixels (not including cloud-covered pixels, lakes or other satellite no data pixels), February 16th snow pillow data for those areas collected, summarized for each 1000' elevation band inside each basin. The last column shows February 16th mean SWE from SNODAS*.*

Basin	Elevation Band	1/29/20 % 2/1 Avg.	2/16/20 % 2/15 Avg.	1/29/20 SWE (in)	2/16/20 SWE (in)	2/16/20 % SCA	2/16/20 Vol (af)	1/29 thru 2/16/20 Chg. in SWE (in)	2/16/20 Area (mi2)	1/29/20 Pillows	2/16/20 Pillows	2/16/20 SNODAS* (in)
Feather	5000-6000'	66	19	5.7	2.2	16.6	157,435	-3.4	1,338.5	21.7 (1)	21.6 (1)	5.6
	6000-7000'	72	43	8.8	6.7	48.5	275,149	-2.1	770.3	15.8 (5)	15.6 (5)	9.2
	7000-8000'	75	65	11.5	13.1	86.6	87,740	1.6	125.9	14.4 (1)	15.1 (1)	13.1
	8000-9000'	70	67	14.3	17.4	98.5	4,389	3.0	4.7	NA	NA	12.9
Yuba	5000-6000'	76	16	7.8	2.0	15.9	21,506	-5.8	200.4	NA	NA	6.3
	6000-7000'	78	59	11.0	10.9	81.9	132,967	-0.1	228.5	17 (2)	17.4 (2)	13.5
	7000-8000'	74	66	12.9	14.8	98.7	92,920	1.8	118.1	23.4 (1)	NA	17.1
	8000-9000'	70	65	15.2	17.8	100.0	4,315	2.6	4.5	NA	NA	19.0
American	5000-6000'	47	14	4.8	1.7	14.0	28,022	-3.1	312.1	4.1 (2)	3.9 (2)	2.1
	6000-7000'	66	57	9.1	9.7	75.7	144,802	0.6	280.8	17.6 (2)	18.4 (2)	8.5
	7000-8000'	74	67	11.6	13.2	96.6	124,068	1.7	175.7	17.6 (3)	17.6 (4)	18.5
	8000-9000'	70	64	13.4	15.5	97.9	58,333	2.1	70.4	19.4 (3)	17.1 (2)	20.0
	9000-10,000'	67	63	15.3	17.8	100.0	8,818	2.5	9.3	NA	NA	17.7
Cosumnes	5000-6000'	5	3	0.3	0.2	2.0	822	0.0	62.8	NA	NA	2.1
	6000-7000'	63	45	7.0	6.3	48.2	8,359	-0.6	24.8	NA	NA	8.0
	7000-8000'	70	71	10.3	13.9	100.0	5,172	3.6	7.0	NA	NA	17.8
Mokelumne	5000-6000'	19	6	1.5	0.6	4.9	2,597	-1.0	87.7	NA	NA	0.6
	6000-7000'	59	45	7.6	7.1	61.2	25,926	-0.5	68.3	NA	NA	6.4
	7000-8000'	72	65	10.9	12.5	98.2	60,642	1.7	90.9	NA	NA	17.5
	8000-9000'	69	64	12.6	14.5	98.6	61,838	1.9	80.1	14.9 (1)	15.9 (1)	18.1
	9000-10,000'	68	64	14.3	16.7	100.0	7,819	2.4	8.8	NA	NA	15.4
Stanislaus	5000-6000'	30	8	2.1	0.7	6.8	4,445	-1.3	112.4	NA	NA	0.6
	6000-7000'	60	49	7.4	7.6	63.7	56,633	0.2	140.5	16.7 (1)	16 (1)	8.1
	7000-8000'	70	62	9.9	11.3	92.2	91,446	1.4	152.4	21.7 (2)	16.9 (1)	14.4
	8000-9000'	68	62	11.7	13.4	99.4	84,448	1.7	118.2	18.4 (2)	18.3 (2)	14.9
	9000-10,000'	66	61	13.5	15.4	99.6	44,418	1.9	54.1	7.3 (1)	7.3 (1)	14.0
	10,000-11,000'	65	61	14.5	16.8	100.0	11,906	2.3	13.3	NA	NA	10.3
	> 11,000'	68	64	14.6	17.4	100.0	259	2.8	0.3	NA	NA	4.4
Tuolumne	5000-6000'	9	1	0.5	0.1	0.7	753	-0.4	179.0	NA	NA	0.2
	6000-7000'	54	32	6.0	4.5	39.0	35,011	-1.6	147.0	6.2 (1)	1.7 (1)	4.7
	7000-8000'	71	59	9.9	10.5	87.1	87,860	0.6	157.3	13.6 (2)	13.3 (2)	13.2
	8000-9000'	68	62	10.6	12.4	97.9	114,279	1.8	173.0	13.7 (2)	14.1 (2)	13.2
	9000-10,000'	63	60	11.6	13.9	98.9	135,464	2.3	183.1	11.2 (2)	12 (2)	14.0
	10,000-11,000'	65	61	12.8	15.0	98.8	73,268	2.2	91.6	NA	NA	10.4
	11,000-12,000'	65	61	12.8	15.4	100.0	21,436	2.6	26.2	NA	NA	4.9
	> 12,000'	67	63	13.5	16.5	100.0	2,518	3.0	2.9	NA	NA	2.5
Merced	5000-6000'	14	1	0.3	0.0	0.4	138	-0.2	74.0	NA	NA	0.3
	6000-7000'	39	17	3.0	1.8	17.9	8,002	-1.2	82.1	NA	NA	4.8
	7000-8000'	67	52	8.3	8.6	78.1	64,760	0.2	141.9	NA	NA	11.0
	8000-9000'	72	60	10.5	11.6	95.9	76,619	1.1	124.2	13.7 (2)	13.4 (2)	11.4
	9000-10,000'	68	59	11.7	13.1	98.4	61,801	1.4	88.3	NA	NA	12.7
	10,000-11,000'	65	59	12.9	14.9	98.1	31,384	2.0	39.6	NA	NA	8.8
	11,000-12,000'	65	61	13.7	16.3	98.2	10,005	2.6	11.5	NA	NA	4.4
	> 12,000'	64	64	14.5	17.9	100.0	1,532	3.4	1.6	NA	NA	3.1

Basin	Elevation Band	1/29/20 % 2/1 Avg.	2/16/20 % 2/15 Avg.	1/29/20 SWE (in)	2/16/20 SWE (in)	2/16/20 % SCA	2/16/20 Vol (af)	1/29 thru 2/16/20 Chg. in SWE (in)	2/16/20 Area (mi2)	1/29/20 Pillows	2/16/20 Pillows	2/16/20 SNODAS* (in)
San Joaquin	5000-6000'	32	1	1.1	0.0	0.5	325	-1.0	144.2	NA	NA	0.9
	6000-7000'	68	18	5.5	2.1	26.0	20,695	-3.4	186.4	9.7 (3)	9.1 (3)	4.4
	7000-8000'	81	39	8.0	5.6	63.7	65,915	-2.5	222.0	10 (3)	10.9 (2)	8.6
	8000-9000'	74	49	9.1	8.4	86.7	91,159	-0.6	202.9	NA	NA	11.4
	9000-10,000'	65	55	10.3	11.2	96.7	123,376	0.9	207.2	10.9 (1)	11.3 (1)	12.5
	10,000-11,000'	62	55	11.1	12.6	97.6	107,976	1.5	160.6	12.7 (1)	11.7 (1)	9.8
	11,000-12,000'	62	58	11.8	13.8	96.6	87,829	2.0	119.3	NA	NA	5.0
	> 12,000'	64	61	12.5	15.2	99.5	22,761	2.7	28.0	NA	NA	2.3
Kings	5000-6000'	64	4	1.5	0.1	2.2	777	-1.4	104.5	NA	NA	0.7
	6000-7000'	84	22	5.1	1.8	24.2	13,095	-3.3	136.3	NA	NA	3.7
	7000-8000'	79	43	7.3	5.6	69.2	52,195	-1.7	175.1	NA	NA	8.6
	8000-9000'	74	51	8.3	8.0	87.0	93,510	-0.3	220.5	NA	NA	12.5
	9000-10,000'	65	53	9.3	10.0	97.0	117,892	0.6	221.3	14.4 (3)	13.8 (3)	13.2
	10,000-11,000'	62	54	9.9	11.1	97.3	114,310	1.2	192.9	13 (3)	12.7 (3)	10.3
	11,000-12,000'	61	57	10.6	12.3	96.4	100,575	1.7	153.1	NA	NA	4.8
	> 12,000'	63	61	11.4	13.9	99.2	39,372	2.5	52.9	NA	NA	2.3
Kaweah	5000-6000'	26	0	0.2	0.0	0.0	0	-0.2	63.4	NA	NA	0.4
	6000-7000'	40	9	1.6	0.6	7.2	1,767	-1.0	59.1	4.9 (1)	2.8 (1)	3.9
	7000-8000'	70	31	5.7	3.6	39.8	11,521	-2.2	60.6	NA	NA	8.9
	8000-9000'	75	45	8.3	7.1	76.4	21,804	-1.2	57.5	NA	NA	13.2
	9000-10,000'	69	52	9.6	9.8	92.7	22,671	0.2	43.4	NA	NA	14.6
	10,000-11,000'	65	56	11.0	12.1	98.7	19,872	1.1	30.7	NA	NA	11.2
	11,000-12,000'	66	57	11.8	13.2	97.6	5,929	1.3	8.4	NA	NA	5.8
	> 12,000'	68	57	11.5	12.5	100.0	140	1.0	0.2	NA	NA	4.2
Tule	5000-6000'	56	0	0.1	0.0	0.0	0	-0.1	55.3	NA	NA	0.1
	6000-7000'	10	2	0.2	0.1	1.3	230	-0.1	41.2	NA	NA	1.3
	7000-8000'	36	22	3.0	2.6	28.9	3,634	-0.4	26.4	9.5 (1)	9.7 (1)	7.2
	8000-9000'	66	29	7.6	4.7	48.1	3,621	-2.9	14.5	NA	NA	11.2
	9000-10,000'	73	49	10.0	9.5	84.6	2,308	-0.4	4.5	NA	NA	13.5
	10,000-11,000'	72	57	10.5	11.3	100.0	84	0.0	0.1	NA	NA	12.1
Kern	5000-6000'	3	0	0.0	0.0	0.0	6	0.0	305.4	NA	NA	0.0
	6000-7000'	28	3	1.2	0.2	3.9	4,431	-1.0	381.7	NA	NA	0.4
	7000-8000'	50	22	4.2	2.3	32.5	42,047	-1.9	348.8	8 (1)	1.1 (1)	2.7
	8000-9000'	62	41	7.1	5.9	77.0	101,988	-1.2	326.1	10.3 (2)	10 (2)	6.0
	9000-10,000'	64	49	8.1	7.9	92.5	81,591	-0.1	192.6	11.1 (1)	13.1 (1)	8.8
	10,000-11,000'	60	52	9.2	10.0	98.4	70,680	0.8	132.6	7.3 (2)	7.6 (2)	7.0
	11,000-12,000'	60	56	10.2	11.7	95.9	57,913	1.5	92.9	6.8 (1)	10.7 (1)	4.5
	> 12,000'	62	60	11.2	13.5	96.4	32,229	2.4	44.6	NA	NA	2.6

Basin	Elevation Band	1/29/20 % 2/1 Avg.	2/16/20 % 2/15 Avg.	1/29/20 SWE (in)	2/16/20 SWE (in)	2/16/20 % SCA	2/16/20 Vol (af)	1/29 thru 2/16/20 Chg. in SWE (in)	2/16/20 Area (mi2)	1/29/20 Pillows	2/16/20 Pillows	2/16/20 SNODAS* (in)
Truckee	5000-6000'	51	15	3.6	1.2	11.5	8,790	-2.3	132.4	NA	NA	0.6
	6000-7000'	57	43	6.9	6.2	55.3	87,653	-0.7	263.9	9.8 (4)	10.3 (4)	6.4
	7000-8000'	70	63	10.2	11.7	89.5	86,163	1.5	138.3	NA	NA	10.5
	8000-9000'	69	66	11.9	14.5	97.9	33,434	2.6	43.4	11 (1)	10.4 (1)	15.0
	9000-10,000'	66	67	12.9	16.8	97.8	8,569	3.9	9.6	NA	NA	16.8
	10,000-11,000'	69	69	15.0	19.0	100.0	423	4.0	0.4	NA	NA	14.0
Tahoe	6000-7000'	53	39	5.0	4.5	18.2	31,726	-0.5	132.6	9.3 (3)	8.7 (3)	4.0
	7000-8000'	66	64	8.1	10.2	85.0	61,779	2.1	113.1	12.8 (4)	13.4 (4)	11.6
	8000-9000'	64	66	10.4	13.9	96.1	53,076	3.5	71.6	9.3 (1)	9.9 (1)	14.5
	9000-10,000'	68	66	13.4	16.3	100.0	14,805	2.9	17.0	NA	NA	13.9
	10,000-11,000'	67	65	14.2	17.2	100.0	767	3.0	0.8	NA	NA	10.7
W. Carson	5000-6000'	0	0	0.0	0.0	0.0	0	0.0	26.8	NA	NA	0.0
	6000-7000'	21	17	1.1	1.1	19.3	834	0.1	13.7	NA	NA	1.1
	7000-8000'	60	62	7.2	9.0	90.1	20,336	1.8	42.4	NA	NA	12.0
	8000-9000'	68	65	10.5	12.5	98.5	24,180	1.9	36.4	14.7 (2)	14.7 (2)	12.5
	9000-10,000'	66	65	12.2	14.8	100.0	9,436	2.6	11.9	NA	NA	12.1
	10,000-11,000'	69	67	12.8	15.8	100.0	998	2.9	1.2	NA	NA	10.5
E. Carson	5000-6000'	2	1	0.1	0.0	0.7	133	0.0	68.8	NA	NA	0.0
	6000-7000'	27	17	1.9	1.4	19.2	7,420	-0.4	96.7	4 (1)	3 (1)	0.8
	7000-8000'	61	56	6.9	7.5	78.0	44,675	0.6	111.5	8.8 (1)	9.6 (1)	6.2
	8000-9000'	66	66	9.9	12.0	98.5	66,522	2.1	103.6	12.6 (3)	12.6 (3)	11.9
	9000-10,000'	65	63	12.1	14.6	99.8	28,304	2.4	36.4	NA	NA	12.7
	10,000-11,000'	65	63	13.7	16.5	100.0	9,556	2.8	10.9	NA	NA	9.9
	> 11,000'	68	65	14.7	18.0	100.0	267	3.2	0.3	NA	NA	7.5
W. Walker	5000-6000'	2	0	0	0	0	0	0.0	81.7	NA	NA	0.0
	6000-7000'	13	2	0.6	0.1	1.3	334	-0.5	72.1	NA	NA	0.1
	7000-8000'	43	25	3.8	2.6	36.6	14,336	-1.2	102.9	6.1 (1)	5.5 (1)	1.4
	8000-9000'	63	55	7.8	8.2	87.5	39,001	0.4	88.8	8.2 (1)	8.6 (1)	4.9
	9000-10,000'	64	61	10.9	12.8	99.3	53,181	2.0	77.7	11.4 (3)	11.9 (3)	11.5
	10,000-11,000'	64	62	12.9	15.5	99.8	25,419	2.6	30.8	NA	NA	9.6
	> 11,000'	68	67	13.4	16.5	100.0	2,518	3.1	2.9	NA	NA	4.8
E. Walker	5000-6000'	0	0	0.0	0.0	0.0	0	0.0	23.2	NA	NA	0.0
	6000-7000'	1	0	0.0	0.0	0.0	0	0.0	222.2	NA	NA	0.0
	7000-8000'	15	6	0.9	0.5	8.6	7,573	-0.4	270.0	NA	NA	0.1
	8000-9000'	48	33	4.8	4.1	49.9	43,143	-0.7	198.4	NA	NA	1.2
	9000-10,000'	62	58	8.5	9.9	90.9	42,913	1.4	81.3	5.2 (1)	5.4 (1)	5.5
	10,000-11,000'	63	64	11.0	13.5	97.9	30,412	2.6	42.2	NA	NA	5.6
	11,000-12,000'	67	68	12.2	15.4	100.0	9,360	3.3	11.4	NA	NA	2.8
	> 12,000'	66	67	12.6	16.0	100.0	238	3.4	0.3	NA	NA	2.2
Mono	6000-7000'	8	0	0.3	0.0	0.9	344	-0.2	321.5	NA	NA	0.0
	7000-8000'	26	6	1.6	0.5	9.8	10,508	-1.1	419.0	NA	NA	0.0
	8000-9000'	48	28	4.5	3.3	49.6	32,934	-1.2	186.8	NA	NA	0.7
	9000-10,000'	59	53	7.5	8.5	91.3	29,301	1.0	64.9	NA	NA	5.3
	10,000-11,000'	61	59	10.2	12.5	96.5	32,115	2.3	48.3	6.9 (1)	6.6 (1)	8.3
	11,000-12,000'	63	62	11.7	14.6	98.7	20,191	2.9	25.9	NA	NA	5.2
	> 12,000'	65	64	12.4	15.6	100.0	3,606	3.2	4.3	NA	NA	2.6
Owens	5000-6000'	0	0	0	0	0	0	0.0	446.9	NA	NA	0.0
	6000-7000'	18	0	0	0	0	44	-0.3	423.1	NA	NA	0.0
	7000-8000'	39	11	1.6	0.7	16.5	18,105	-0.9	485.5	NA	NA	0.3
	8000-9000'	43	24	2.5	1.9	43.7	27,483	-0.5	268.8	NA	NA	2.4
	9000-10,000'	50	35	4.3	3.9	68.9	40,443	-0.4	196.5	7.6 (3)	8.5 (3)	4.7
	10,000-11,000'	56	48	6.6	7.2	87.5	77,249	0.6	201.6	7.5 (2)	7.2 (2)	5.1
	11,000-12,000'	58	55	8.6	10.0	92.7	79,866	1.4	149.8	NA	NA	3.3
	> 12,000'	61	60	10.1	12.4	94.0	52,881	2.3	80.1	NA	NA	1.9

* This is a comparison to the SNODAS (SNOw Data Assimilation System) nationwide product from the National Weather Service.

Location of Reports and Excel Format Tables

ftp://snowserver.colorado.edu/pub/fromLeanne/forCADWR/Near_Real_Time_Reports/

References and Additional Sources

Margulis, S. A., Cortés, G., Girotto, M., & Durand, M. (2016). A Landsat-Era Sierra Nevada Snow Reanalysis (1985–2015). *Journal of Hydrometeorology*, 17(4), 1203–1221, doi:/10.1175/JHM-D-15-0177.1

Painter, T.H., K. Rittger, C. McKenzie, P. Slaughter, R. E. Davis and J. Dozier. (2009) Retrieval of subpixel snow covered area, grain size, and albedo from MODIS. *Remote Sensing of the Environment*, 113: 868-879.

Schneider D. and N.P. Molotch. (2016). Real-time estimation of snow water equivalent in the Upper Colorado River Basin using MODIS-based SWE reconstructions and SNOTEL data. *Water Resources Research*, 52(10): 7892-7910. DOI: 10.1002/2016WR019067.

Molotch, N.P. (2009). Reconstructing snow water equivalent in the Rio Grande headwaters using remotely sensed snow cover data and a spatially distributed snowmelt model. *Hydrological Processes*, Vol. 23, doi: 10.1002/hyp.7206, 2009.

Molotch, N.P., and S.A. Margulis. (2008) Estimating the distribution of snow water equivalent using remotely sensed snow cover data and a spatially distributed snowmelt model: a multi-resolution, multi-sensor comparison. *Advances in Water Resources*, 31, 2008.

Molotch, N.P., and R.C. Bales. (2006). Comparison of ground-based and airborne snow-surface albedo parameterizations in an alpine watershed: impact on snowpack mass balance. *Water Resources Research*, VOL. 42, doi:10.1029/2005WR004522.

Molotch, N.P., and R.C. Bales. (2005). Scaling snow observations from the point to the grid-element: implications for observation network design. *Water Resources Research*, VOL. 41, doi: 10.1029/2005WR004229.

Molotch, N.P., T.H. Painter, R.C. Bales, and J. Dozier. (2004). Incorporating remotely sensed snow albedo into a spatially distributed snowmelt model. *Geophysical Research Letters*, VOL. 31, doi:10.1029/2003GL019063, 2004.